Asian Journal of Chemistry; Vol. 35, No. 3 (2023), 748-754

ASIAN JOURNAL OF CHEMISTRY

https://doi.org/10.14233/ajchem.2023.27590

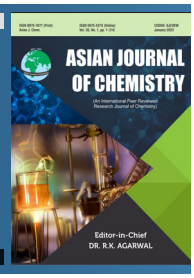

Optimized Geometry, NBO, MEP, Docking Analysis and Antimicrobial Activity of (2*R*,3*R*)-Butanediol *Bis*(methanesulfonate)

P.R. Babila*, G. Edwin Sheela and E.S. Ashlin

Department of Physics and Research Centre, Muslim Arts College (Affiliated to Manonmaniam Sundaranar University, Tirunelveli), Thiruvinthancode-629174, India

*Corresponding author: E-mail: prbabila@gmail.com

Received: 3 January 2023; *Accepted*: 20 February 2023; *Published online*: 27 February 2023; AJC-21171

In this work, quantum chemical computations using density functional theory (DFT) with the wB97XD basis functional were used to characterize (2*R*,3*R*)-butanediol *bis*(methanesulfonate) (BBM). Natural bond orbital analysis was used to examine the electronic chemical stability of the BBM induced by hyperconjugative interactions and charge delocalization. The compound is chemically active and the atomic sites prone to electrophilic/nucleophilic attack were recognized form molecular electrostatic potential (MEP) surface. Molecular docking studies were on four (*Candida albicans*, *Aspergillus niger*, *Bacillus cereus* and *Pseudomonas aeruginosa*) organisms PDB antibacterial proteins and higher binding energy and lower inhibition constants of the docked complex were endorsed the inhibition activity of BBM against the 5DXF, 1UKC, 4NQ6 and 4LJH targets. *In vitro* analysis had also performed with two antimicrobial pathogens *viz*. *Candida* sp. and *E. coli*.

Keywords: (2*R*,3*R*)-butanediol *bis*(methanesulfonate), molecular electrostatic potential surface, *Candida* sp., *E. coli*.

INTRODUCTION

In the last decades, several alkylsulfonate derivatives were examined by pollsters in the spectroscopic and therapeutic field due to their incredible pharmacological and biological activities [1]. In therapeutic, several varieties of approaches for treating chronic myeloid leukaemia (CML). However, alkylsulfonate is governed in words and it sources less nausea and vomiting than other DNA crosslinking agents. Maintaining patients in a nearly symptom-free state for extended periods of time is, thus, of great value and insight [2]. Alkylsulfonates are approved by USFD administration for the treatment of chronic myeloid leukemia [3].

(2*R*,3*R*)-Butanediol *bis*(methanesulfonate) (BBM) is an alkylsulfonate crosslinking agent and its interaction with DNA has explained by alkylating DNA crosslinking agents through the molecular electrostatic potential surface analysis [4]. The quantum chemical and docking methods were used to explain the biological activities of alkylsulfonates in the context of their electronic and molecular structures, reactivity and drug-enzyme binding [5]. The computational predictions of active binding sites on specific biological targets against BBM have also been reported [3]. When this molecule interacts with a protein, the methanesulfonate groups, which are attached to the two ends of the alkyl chain, are released resulting in the formation of carbonium ions through hydrolysis [6]. The intramolecular hydrogen bonding interactions in the conformers of alkyl-sulfonates were identified as the active binding sites on selected biological targets for alkylsulfonates [7].

According to the literature review, no studies have been conducted on (2*R*,3*R*)-butanediol *bis*(methanesulfonate) (BBM) molecule's conformational geometry, NBO analysis, molecular electrostatic potential (MEP) surface studies and molecular docking. Hence, in present work, the optimized geometrical parameters of BBM molecule were analyzed. Moreover, molecular electrostatic potential (MEP) surface is plotted over the optimized geometry to explicate the reactivity of BBM molecule. The redistribution of electron density (ED) in various bonding and anti-bonding orbital and hyper conjugation energies of BBM were calculated by natural bond orbital (NBO) analysis. The docking method was used to assess the biological activities of the BBM molecule and its antimicrobial activity was also studied.

EXPERIMENTAL

A pure sample of (2*R*,3*R*)-butanediol *bis*(methanesulfonate) (BBM) molecule was purchased from Sigma-Aldrich, USA. After inoculation, a sterile cork borer was used to create wells in each of these plates, each measuring 10 mm in diameter and arranged about 2 cm apart. Extracts from each drug were diluted to 1 mg/mL stock solution in water. For this experiment, approximately 100 µL of various solvent extract concentrations to the wells and let them diffuse at room temperature for 2 h. For 24 h, the plates were incubated at 37 ºC and then the activity index and the diameter of the inhibition zone were measured.

Computational details

Quantum chemical computations: The electronic structure of (2*R*,3*R*)-butanediol *bis*(methanesulfonate) (BBM) is provided by the pubchem database and optimized wB97XD/6-311++G (d,p) level of approximations using Gaussian 09W software [8,9]. Hence, they are accurately predicting the minimum energy structure [10]. The second order perturbation energies from donor and acceptor species of BBM molecule were predicted using NBO 3.1 program at wB97XD and camB3LYP DFT functional with 6-311++G(d,p) basis set combinations. Molecular electrostatic potential (MEP) of BBM molecules have been performed by Gauss View 5.0 [11].

Molecular docking: The molecule (BBM) was docked with the selected organism PDB antibacterial proteins using the AutoDock4.2 software packages [12] and the docking results were analyzed and visualized using Pymol software [13]. To further understand the binding characteristics of alkylsulfonates, molecular docking studies were conducted. For preparing the targets, the Auto Dock Tool (ADT) graphical user interface (GUI) was used and predefined scripts for adding the hydrogen atoms, by removal of water molecules and Kollmann charges to the residues. The ligand structure optimized to minimum energy at wB97XD/6-311++G (d,p) level of theory was introduced and the conformation detection roots were identified using ADT script. The Lamarckian genetic algorithm procedure was used, which was implemented in the Auto Dock software. Each enzyme had a search region (docking grid box) with a grid size 60 Å × 60 Å × 60 Å covered the active site of enzyme. The dimensions of box were such that the whole working space was contained within them. Molecule was docked in the functional areas of the protein of concern was performed in 10 separate runs, with each run beginning with a random set and the minimal docking energy value was determined. The docked conformation with the lowest binding energy was selected to investigate the binding mode of the molecules.

RESULTS AND DISCUSSION

Geometricl parameters: The optimized structure of the BBM molecule was obtained by using quantum chemical computations at DFT/wB97XD/6-311++G (d,p) basis set (Fig. 1). Table-1 displays the results of a comparison between the theoretical and experimental values for the geometric parameters of the BBM molecule. In BBM molecule, three C-C bond lengths, fourteen C-H bond lengths, two C-O bond lengths, six S-O bond lengths and two S-C bond lengths. The three C-C bond lengths of BBM are smaller than the normal C-C single bond of 1.54 Å [14]. The C-O bond lengths by DFT/wB97XD/6-311++G(d,p) in the range of 1.42 Å, it is nearly closest for experimental value. The oxidation of BBM molecule occurs at the C-O bonds and provides a plethora of data about the

TABLE-1
GEOMETRICAL PARAMETERS OF (2*R*,3*R*)-BUTANEDIOL *BIS*(METHANESULFONATE) (BBM)

Bond lengths	Calcd. (Å)	Expt. (Å)	Bond angles	Calcd. (°)	Expt. (°)	Dihedral angles	Calcd. (°)	Expt. (°)
S_1-O_3	1.6191	1.631	O_3-S_1-O_6	109.0	109.46	O_6-S_1-O_3-C_{10}	91.2	88.08
S_1-O_6	1.4456	1.449	O_3-S_1-O_7	108.2	109.47	S_1-O_3-C_{10}-H_{16}	38.5	38.99
S_1-O_7	1.4457	1.449	O_3-S_1-C_{14}	97.0	96.53	S_2-O_4-C_9-C_{10}	152.8	156.12
S_1-C_{14}	1.7749	1.775	O_6-S_1-O_7	119.0	122.03	S_2-O_4-C_9-C_{12}	-82.4	-80.00
S_2-O_4	1.6191	1.630	O_6-S_1-C_{14}	110.2	108.16	S_2-O_4-C_9-H_{15}	38.5	38.26
S_2-O_5	1.4456	1.449	O_4-S_2-C_{13}	97.0	96.54	O_4-C_9-C_{10}-O_3	67.6	63.38
S_2-O_8	1.4457	1.449	O_5-S_2-O_8	119.4	122.02	C_{12}-C_9-C_{10}-O_3	-54.7	-58.00
S_2-C_{13}	1.7749	1.775	O_8-S_2-C_{13}	110.3	108.13	C_{12}-C_9-C_{10}-C_{11}	-177.1	-178.84
O_3-C_{10}	1.4548	1.426	S_1-O_3-C_{10}	116.6	118.53	C_{12}-C_9-C_{10}-H_{16}	60.1	61.27
O_4-C_9	1.4548	1.426	O_4-C_9-C_{12}	108.5	108.41	H_{15}-C_9-C_{10}-O_3	-178.6	-177.37
C_9-C_{10}	1.5221	1.535	C_{10}-C_9-H_{15}	106.4	107.24	H_{15}-C_9-C_{10}-C_{11}	60.1	61.79
C_9-C_{12}	1.5132	1.524	C_{10}-C_9-C_{12}	114.2	112.69	H_{15}-C_9-C_{10}-H_{16}	-62.8	-58.10
C_9-H_{15}	1.0950	1.097	O_3-C_{10}-C_{11}	108.5	108.65	O_4-C_9-C_{12}-H_{20}	-56.6	-52.93
C_{10}-C_{11}	1.5132	1.524	C_9-C_{10}-C_{11}	114.2	112.36	O_4-C_9-C_{12}-H_{21}	63.6	65.91
C_{10}-H_{16}	1.0955	1.097	C_{10}-C_{11}-H_{17}	110.2	111.28	O_4-C_9-C_{12}-H_{22}	-176.6	-174.26
C_{11}-H_{17}	1.0904	1.096	C_{10}-C_{11}-H_{19}	109.6	110.97	C_{10}-C_9-C_{12}-H_{20}	63.7	69.57
C_{11}-H_{18}	1.0923	1.094	H_{17}-C_{11}-H_{18}	108.9	108.79	C_{10}-C_9-C_{12}-H_{21}	-176.2	-171.09
C_{11}-H_{19}	1.0905	1.094	H_{17}-C_{11}-H_{19}	108.6	106.71	C_{10}-C_9-C_{12}-H_{22}	-56.3	-51.76
C_{12}-H_{20}	1.0891	1.095	H_{18}-C_{11}-H_{19}	108.4	107.78	H_{15}-C_9-C_{12}-H_{20}	-176.5	-117.82
C_{12}-H_{21}	1.0905	1.094	C_9-C_{12}-H_{20}	110.2	111.25	O_3-C_{10}-C_{11}-H_{17}	-56.5	-52.50
C_{12}-H_{22}	1.0923	1.095	C_9-C_{12}-H_{21}	110.6	111.06	O_3-C_{10}-C_{11}-H_{18}	-176.6	-173.91
C_{13}-H_{23}	1.0878	1.092	C_9-C_{12}-H_{22}	109.8	111.13	O_3-C_{10}-C_{11}-H_{19}	63.6	66.17
C_{13}-H_{24}	1.0896	1.092	H_{20}-C_{12}-H_{22}	108.0	108.75	C_9-C_{10}-C_{11}-H_{17}	63.7	68.84
C_{13}-H_{25}	1.0878	1.092	S_2-C_{13}-H_{24}	106.1	108.12	C_9-C_{10}-C_{11}-H_{18}	-56.3	-52.56

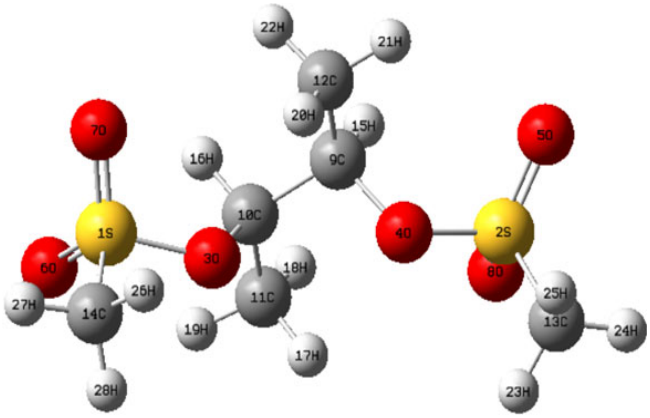

Fig. 1. Optimized structure of (2*R*,3*R*)-butanediol *bis*(methanesulfonate)

biological properties of molecule. Since like charges repel one other and unlike charges attract each other, homonuclear bond lengths are larger than heteronuclear bond lengths [15].

NBO analysis: The natural bond orbital calculations were performed on the titled compound (BBM) to explicate the possible charge delocalization between the donor (lone pair, bonding) and acceptor (anti-bonding) orbital. The electron occupancy of bonding (σ), anti-bonding (σ*) and lone pair (n) orbital of the BBM molecule were to explore the bond order between the atoms and the strength of non-covalent interactions, *etc*. A DFT theory at wB97XD/6-311++G(d,p) and cam-B3LYP/6-311++G (d,p) basis functional were implemented for NBO analysis. The stabilization energy $E^{(2)}$ associated with various donors orbital (i) and acceptor orbital (j) were calculated [16] and the results are presented in Table-2.

The occupancy of electrons and energy on n, σ and σ* orbital of BBM molecule on both sides of bond S-O in wB97XD and cam-B3LYP levels were found to be equal. This indicates both the achiral nature of the stereogenic axis along the S-O bond and a high degree of symmetry [17]. The occupancies and the energies of certain NBOs, which are prone to charge delocalization are presented in Table-3.

The prominent stabilization energy of about 43 kcal/mol was obtained for the interactions n3 (O_5) → σ*(S_2-O_4), n3 (O_7) → σ*(S_1-O_3) and n3 (O_8) → σ*(S_2-O_4) at wB97XD/6-311++G (d,p) level. These interactions give strong stabilization to the molecule. Occupancy of the C-C sigma bonds is nearly equal to 1.97e for both wB97XD and cam-B3LYP levels, which are sp^3 hybridized [18]. The compositions of H-bonded NBO in terms of natural atomic hybrid are shown in Table-4.

Hybrids related to central carbon atoms S_2-C_{13} and O_3-C_{10} were protonated $sp^{2.82}$ and $sp^{2.78}$ by forming the NBOs of the BBM molecule. The O_3-C_{10} hybrid orbital of the *s*-character $sp^{2.01}$ enables the O_3-C_{10} bond to become significantly more stable [19]. A C_{11}-H_{19} bond at C_{11} through $sp^{3.16}$ hybridization in BBM molecule confirms that the acidity of the donor C-H group, as well as its potential hydrogen bond strength, increases while changing the hybridization of C atoms from sp^2 to *sp* and is further elevated by the surrounding electron withdrawing atoms.

Molecular electrostatic potential (MEP) surface studies: Predicting the reactive charges of electrophilic and nucleophilic reaction for the study of intermolecular hydrogen bonding contact is significantly assisted by using the MEP, which is built with the region around the molecule due to the species distribution [20]. Table-5 listed the calculated electrostatic point charges (e) and electrostatic potential V(r) values on the specific atoms as a result of the charge distribution.

MEP generally allows to shows the charged regions of a molecule in terms of colour grading. The presence of electrophilic and nucleophilic sites can be predicted accurately using this method. There is a positive potential for free neutral atoms, and it is maximum in the nucleus [21]. In BBM molecule shows the electronegativity oxygen atoms represents red region and methyl group and sulfur atoms indicates the electropositive blue region. Based on these findings, it is clear that the comp-

TABLE-2
SECOND ORDER PERTURBATION THEORY ANALYSIS OF FOCK MATRIX OF BBM IN NBO BASIS

Donor $NBO_{(i)}$	Acceptor $NBO_{(j)}$	DFT/wB97XD/6- 311++G(d,p)		DFT/cam-B3LYP/6-311++G (d,p).	
		$E^{(2)}$ (kcal/mol)	$E_{(j)}$-$E_{(i)}$ (a.u.)	$E^{(2)}$ (kcal/mol)	$E_{(j)}$-$E_{(i)}$ (a.u.)
σ (S_1-O_6)	σ* (S_1-O_6)	0.51	1.48	0.54	1.45
n2 (O_8)	σ*(C_{13}-H_{25})	0.82	0.83	0.65	0.80
n1(O_3)	σ*(C_{14}-H_{27})	0.83	1.19	0.59	1.14
n2(O_3)	σ*(C_{11}-H_{18})	0.94	0.93	0.82	0.89
σ (C_9-C_{10})	σ*(S_1-O_3)	1.31	0.9	2.32	0.86
σ (S_1-O_3)	σ*(S_1-O_3)	1.90	1.10	1.90	1.10
σ (C_9-C_{12})	σ*(C_{10}-C_{11})	2.46	1.2	2.42	1.16
σ (S_1-C_{14})	σ*(S_1-O_3)	3.38	0.95	3.11	0.91
σ (S_2-C_{13})	σ*(S_2-O_4)	3.4	0.95	3.11	0.91
n2(O_3)	σ*(C_{10}-C_{11})	4.9	0.91	5.81	0.87
σ (C_{11}-H_{18})	σ*(O_3-C_{10})	6.72	0.89	6.41	0.87
n2(O_3)	σ*(S_1-O_6)	8.04	0.81	10.62	0.77
n2(O_5)	σ*(S_2-C_{13})	16.07	0.58	19.45	0.54
n2 (O_8)	σ*(S_2-O_5)	25.53	0.75	23.80	0.72
n2(O_7)	σ*(S_1-O_6)	25.56	0.75	23.80	0.72
n3(O_5)	σ*(S_2-O_4)	43.21	0.53	40.33	0.49
n3(O_8)	σ*(S_1-O_4)	43.73	0.53	39.39	0.5
n3(O_7)	σ*(S_1-O_3)	43.74	0.53	39.39	0.5

TABLE-3
OCCUPANCY OF THE INTERACTING NBOs WITH THEIR CORRESPONDING ENERGIES OF BBM MOLECULE

Parameters	Occupancy (e)		Δocc(e)	Energy (kcal/mol)		ΔE (kcal/mol)
	wB97XD	cam-B3LYP		wB97XD	cam-B3LYP	
σ (S_1-C_{14})	1.9737	1.9744	0.0007	-0.8045	-0.7900	0.0145
σ (C_9-C_{10})	1.9782	1.9738	0.0044	-0.7494	-0.7355	0.0139
σ (C_9-H_{15})	1.9717	1.9710	0.0007	-0.6230	-0.6044	0.0186
n1(O_3)	1.9630	1.9612	0.0018	-0.7500	-0.7186	0.0314
n2(O_5)	1.8124	1.8122	0.0002	-0.3826	-0.3704	0.0122
n3(O_6)	1.7804	1.7787	0.0017	-0.3804	-0.3659	0.0145
σ*(S_1-C_{14})	0.1603	0.1574	0.0029	0.1927	0.1732	0.0195
σ*(S_2-O_8)	0.1451	0.1401	0.005	0.3618	0.3357	0.0261
σ*(O_3-C_{10})	0.0480	0.0466	0.0014	0.3011	0.2805	0.0206
σ*(C_9-C_{10})	0.0369	0.0336	0.0033	0.4417	0.4210	0.0207
σ*(C_{10}-H_{16})	0.0234	0.0248	0.0014	0.4578	0.4439	0.0139
σ*(C_{11}-H_{18})	0.0047	0.0053	0.0006	0.4882	0.4567	0.0315
σ*(C_{13}-H_{24})	0.0042	0.0048	0.0006	0.4441	0.4238	0.0203
σ*(C_{14}-H_{28})	0.0072	0.0069	0.0003	0.4508	0.4297	0.0211

TABLE-4
COMPOSITION OF H-BONDED NBO IN TERMS OF NATURAL ATOMIC HYBRIDS

Bond (A-B)	B97XD						
	ED		sp^n	A		B	
	A (%)	B (%)		s (%)	p (%)	s (%)	p (%)
S_1-O_3	30.6	69.4	$sp^{4.14}$	19.0	78.6	18.4	81.5
S_2-C_{13}	49.9	50.1	$sp^{2.82}$	25.8	72.8	20.3	79.4
O_3-C_{10}	70.2	29.8	$sp^{2.01}$	33.2	66.8	17.6	82.1
C_{11}-H_{19}	61.2	38.8	$sp^{3.16}$	24.1	75.9	99.9	0.3

TABLE-5
MEP ANALYSIS USING wB97XD BASIS SET OF BBM MOLECULE

Atoms	Charge (e)	V(r) (a.u.)	Atoms	Charge (e)	V(r) (a.u.)	Atoms	Charge (e)	V(r) (a.u.)
S_1	1.2063	-58.9960	C_{11}	-0.4049	-14.7724	H_{20}	0.1371	-1.1110
S_2	1.2081	-58.9961	C_{12}	-0.4416	-14.7724	H_{21}	0.1371	-1.1101
O_3	-0.4772	-22.3083	C_{13}	-0.4839	-14.7172	H_{22}	0.1225	-1.1048
O_4	-0.4750	-22.3083	C_{14}	-0.4804	-14.7172	H_{23}	0.1778	-1.0528
O_5	-0.5586	-22.3668	H_{15}	0.0234	-1.0786	H_{24}	0.1847	-1.0501
O_6	-0.5580	-22.3668	H_{16}	0.0213	-1.0786	H_{25}	0.1769	-1.0534
O_7	-0.5633	-22.3668	H_{17}	0.1280	-1.1110	H_{26}	0.1769	-1.0528
O_8	-0.5644	-22.3668	H_{18}	0.1118	-1.1048	H_{27}	0.1836	-1.0500
C_9	0.3565	-14.6809	H_{19}	0.1278	-1.1101	H_{28}	0.1764	-1.0534
C_{10}	0.3513	-14.6808	–	–	–	–	–	–

ound interacted with the biological molecules at the molecular level [22]. From MEP (Fig. 2), the oxygen atoms (O_3, O_4, O_5, O_6, O_7 and O_8) attached to sulfur atoms (S_1 and S_2) are electrophilic in nature. Since the electropositive atoms S_1 and S_2 are linked with three electronegative oxygen atoms, and the surrounding surfaces appear to be red. The cloud charge transfer was occurred between the ranges of -4.533 e^{-2} to 4.533 e^{-2} on the wB97XD-basis set.

The electrostatic potential values of the atoms S_1 and S_2 calculated by wB97XD basis set were 58.9960 a.u. Also, the atom H_{18} is reported to have a lower positive electrostatic point charge of 0.1118, which shows the less electronegative nature of atoms. The atom O_5 has a lower negative electrostatic point charge of –0.5586, demonstrating that less electropositive atoms tend to have lower values for this property.

Molecular docking: Drug discovery now heavily relies on the capacity to predict the chemical interactions between the active compounds and targets (proteins displaying biological activity). Moreover, the chemical processes and selectivity can be uncovered through docking studies of the lead compound with many protein targets [23]. The protein was prepared for docking by eliminating the water molecules. The docking protocol anticipated the same conformation within the acceptable range of 2 Å [24]. The binding energy of BBM molecule with antibacterial proteins were 5DXF, 1UKC, 4NQ6 and 4LJH were calculated as -5.65, -5.22, -4.92 and -3.83 kcal/mol.

The non-bonding interactions, such van der Waals and hydrophobic contacts can be explained through stability of the binding energy. Comparing all the proteins docked with BBM molecule, the 4NQ6 protein has lowered the inhibition

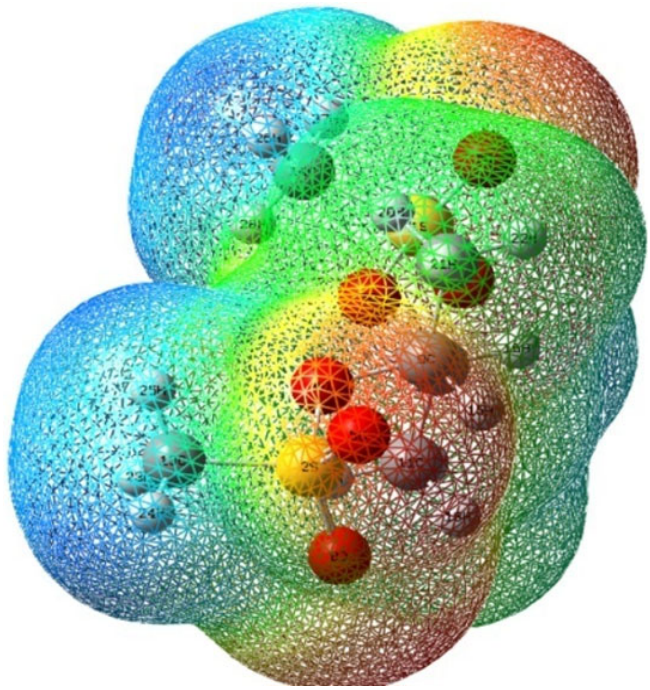

Fig. 2. MEP of (2*R*,3*R*)-butanediol *bis*(methanesulfonate) molecule

constant of 248.58 μM. It has been predicted more biological activity than the other studied proteins. Table-6 shows docking parameters using AutoDock of BBM molecule, whereas Fig. 3 shows the docked molecule of BBM with antibacterial protein.

Antimicrobial activity: The antimicrobial activities of BBM molecule against for fungal and bacterial strains are listed in Table-7. Based on the results, it is established that the BBM molecule has nearly the same antifungal activity against Candida sp. as comparable to standard drug ketoconazole, and that it also has nearly the same antibacterial activity against *E. coli* as comparable to standard drug cotrimoxazole.

Conclusion

In this work, quantum chemical computations were used to perform a thorough analysis of the optimized geometry on the structure, natural bond orbital analysis of (2*R*,3*R*)-butanediol *bis*(methanesulfonate) (BBM). The optimized geometry calculations of BBM molecule were based on DFT/wB97XD basis set, which shows the influence of long range interactions. Molecular electrostatic potential (MEP) predicts the reactive region of the BBM molecule and that region shows the intermolecular interactions with the biological molecules. The prominent stabilization energy of approximately 43 kcal/mol were

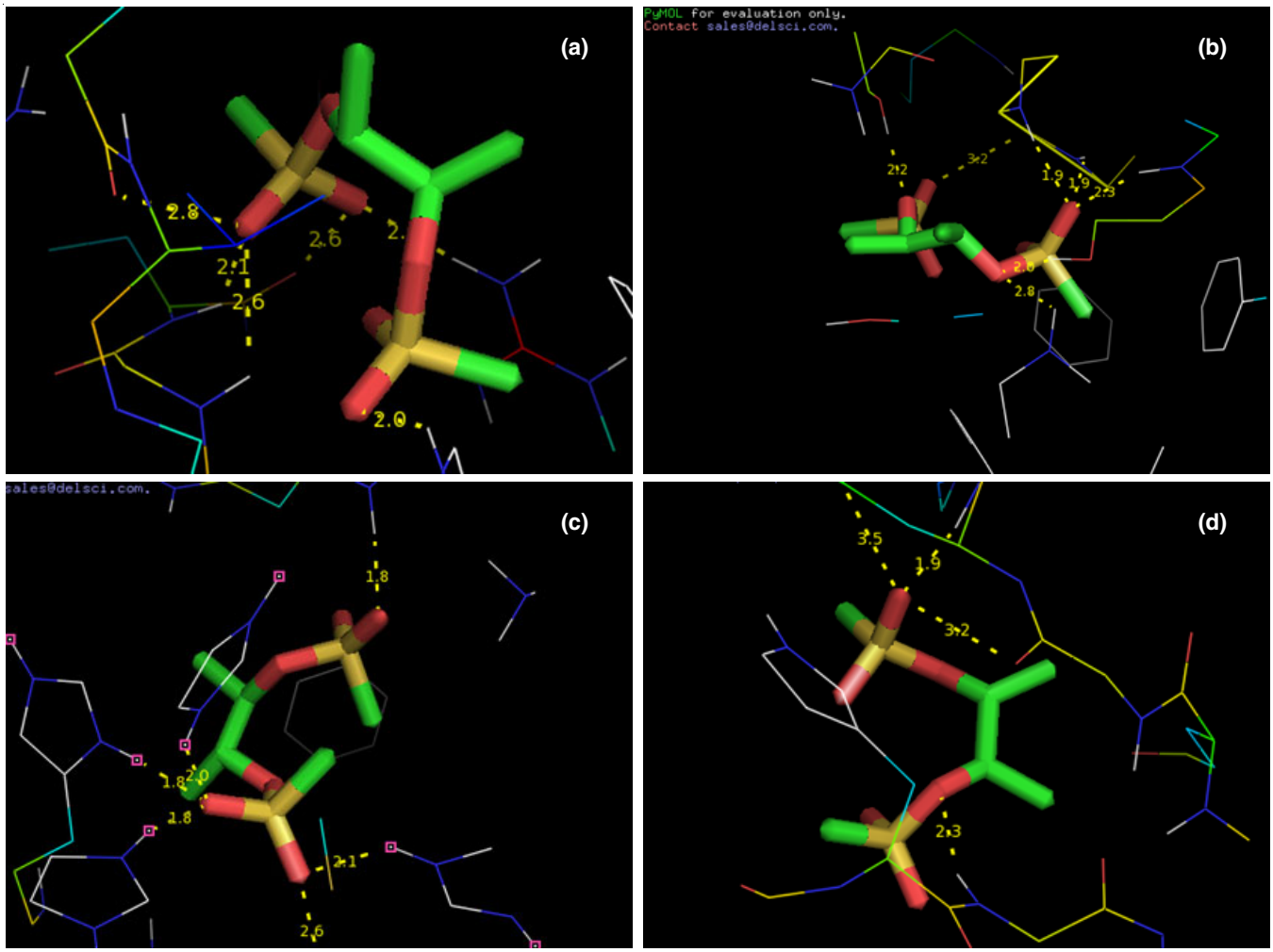

Fig. 3. Docked protein (2*R*,3*R*)-butanediol *bis*(methanesulfonate)

TABLE-6
DOCKING PARAMETERS OF (2*R*,3*R*)-BUTANEDIOL *BIS*(METHANESULFONATE)

Protein (PDB ID)	Type of organism	Bonded residues	Bond distance (Å)	Inhibition constant (μM)	Binding energy (kcal/mol)
5DXF	*Candida albicans*	HIS'229 HIS'161 MET'437 ARG'344 MET'437 GLY'436	2.8 2.0 2.6 2.0 2.1 2.6	72.27	-5.65
1UKC	*Aspergillus niger*	HIS'440 SER'133 GLY'127 SER'210 ALA'211 GLY'128 GLY'127	2.8 2.2 3.2 2.0 2.3 1.9 1.9	148.03	-5.22
4NQ6	*Bacillus cereus*	ASN'180 HIS'210 ASP'90 HIS'149 HIS'88 HIS'86	1.8 2.1 2.6 2.0 1.8 1.8	248.58	-4.92
4LJH	*Pseudomonas aeruginosa*	ASP'47 ARG'48 GLY'46 GLY'43	3.5 1.9 3.2 2.3	1.57 mM	-3.83

TABLE-7
ANTIMICROBIAL ACTIVITY OF PLANT EXTRACT AGAINST FOR FUNGAL AND BACTERIAL STRAINS OF (2*R*,3*R*)-BUTANEDIOL *BIS*(METHANESULFONATE)

Pathogens	Zone of inhibition (mm) at 30 μL	
	Positive control (mm)	Size of inhibition (mm)
Candida sp.	25	23
Escherichia coli	23	21

obtained for the interactions n3 (O_5) → σ*(S_2-O_4), n3 (O_7) → σ*(S_1-O_3) and n3 (O_8) → σ*(S_2-O_4). The binding energy of the BBM molecule with the 5DXF protein was determined to be -5.65 kcal/mol during the docking method, indicating the more enhanced the antibacterial interaction. In antimicrobial activity of BBM molecule against the fungal and bacterial strains molecule shows the enhanced activity.

ACKNOWLEDGEMENTS

The authors acknowledge the opportunity to do the computational work in the Research Lab at Department of Physics, University of Kerala, which was generously provided by Prof. Dr. I. Hubert Joe.

CONFLICT OF INTEREST

The authors declare that there is no conflict of interests regarding the publication of this article.

REFERENCES

1. U. Salar, K.M. Khan, S.A. Ejaz, A. Hameed, M. Al-Rashida, S. Perveen, M.N. Tahir, J. Iqbal and M. Taha, *Lett. Drug Design Discov.*, **16**, 256 (2019); https://doi.org/10.2174/1570180815666180327125738
2. R. Mckenna, S. Neidle, R. Kuroda and B.W. Fox, *ActaCryst.*, **C45**, 311 (1989); https://doi.org/10.1107/S0108270188011291
3. T. Karthick and P. Tandon, *J. Mol. Model.*, **22**, 142 (2016); https://doi.org/10.1007/s00894-016-3015-z
4. V. Kumar, G. Jain, S. Kishor and L.M. Ramaniah, *Comput. Theor. Chem.*, **968**, 18 (2011); https://doi.org/10.1016/j.comptc.2011.04.034
5. I. Novak and B. Kovac, *Chem. Phys. Lett.*, **498**, 240 (2010); https://doi.org/10.1016/j.cplett.2010.08.073
6. T. Iwamoto, Y. Hiraku, S. Oikawa, H. Mizutani, M. Kojima and S. Kawanishi, *Cancer Sci.*, **95**, 454 (2004); https://doi.org/10.1111/j.1349-7006.2004.tb03231.x
7. T. Karthick, P. Tandon, S. Singh, P. Agarwal and A. Srivastava, *Spectrochim. Acta A Mol. Biomol. Spectrosc.*, **173**, 390 (2017); https://doi.org/10.1016/j.saa.2016.09.031
8. M. Beytur and I. Avinca, *Heterocycl. Commun.*, **27**, 1 (2021); https://doi.org/10.1515/hc-2020-0118
9. M.J. Frisch, G.W. Trucks, H.B. Schlegel, G.E. Scuseria, M.A. Robb, J.R. Cheeseman, G. Scalmani, V. Barone, G.A. Petersson, H. Nakatsuji, X. Li, M. Caricato, A. Marenich, J. Bloino, B.G. Janesko, R. Gomperts, B. Mennucci, H.P. Hratchian, J.V. Ortiz, A.F. Izmaylov, J.L. Sonnenberg, D. Williams-Young, F. Ding, F. Lipparini, F. Egidi, J. Goings, B. Peng, A. Petrone, T. Henderson, D. Ranasinghe, V.G. Zakrzewski, J. Gao, N. Rega, G. Zheng, W. Liang, M. Hada, M. Ehara, K. Toyota, R. Fukuda, J. Hasegawa, M. Ishida, T. Nakajima, Y. Honda, O. Kitao, H. Nakai, T. Vreven, K. Throssell, J.A. Montgomery, Jr., J.E. Peralta, F. Ogliaro, M. Bearpark, J.J. Heyd, E. Brothers, K.N. Kudin, V.N. Staroverov, T. Keith, R. Kobayashi, J. Normand, K. Raghavachari, A. Rendell, J.C. Burant, S.S. Iyengar, J. Tomasi, M. Cossi, J.M. Millam, M. Klene, C. Adamo, R. Cammi, J. W. Ochterski, R.L. Martin, K. Morokuma, O. Farkas, J.B. Foresman and D. J. Fox, Gaussian, Inc., Wallingford CT (2016).
10. A.D. Becke, *J. Chem. Phys.*, **98**, 5648 (1993); https://doi.org/10.1063/1.464913
11. R. Dennington, T. Keith and J. Millam, GaussView, Semichem Inc., Shawnee Mission, KS, Version 5 (2009).
12. F. Biegler-Konig, J. Schonbohm and D. Bayles, *J. Comput. Chem.*, **22**, 545 (2001); https://doi.org/10.1002/1096-987X(20010415)22:5<545::AID-JCC1027>3.0.CO;2-Y

13. T. Lu and F. Chen, *J. Comput. Chem.*, **33**, 580 (2012); https://doi.org/10.1002/jcc.22885
14. Y.S. Beegum, S. Mary, Y.S. Mary, R. Thomas, S. Armakovic, S.J. Armakovic, J. Zitko, M. Dolezal and C. van Alsenoy, *Spectrochim. Acta A Mol. Biomol. Spectrosc.*, **24**, 117414 (2019); https://doi.org/10.1016/j.saa.2019.117414
15. F. Weinhold and E.D. Glendening, *J. Phys. Chem. A*, **122**, 724 (2018); https://doi.org/10.1021/acs.jpca.7b08165
16. D. Nasipuri, Stereochemistry of Organic Compounds: Principles and Applications, New Age International Publications: New Delhi, India, Edn. 2 (2005).
17. V. Balachandran, S. Rajeswari and S. Lalitha, *J. Mol. Struct.*, **1007**, 63 (2012); https://doi.org/10.1016/j.molstruc.2011.10.014
18. S.J.J. Mary, M.U.M. Siddique, S. Pradhan, V. Jayaprakash and C. James, *Spectrochim. Acta A Mol. Biomol. Spectrosc.*, **244**, 118825 (2021); https://doi.org/10.1016/j.saa.2020.118825
19. A.A. Bunaciu and H.Y. Aboul-Enein, Encyclopedia of Spectroscopy and Spectrometry, pp. 575-581 (2017).
20. P. Agarwal, S. Bee, A. Gupta, P. Tandon, V.K. Rastogi, S. Mishra and P. Rawat, *Spectrochim. Acta A Mol. Biomol. Spectrosc.*, **121**, 464 (2014); https://doi.org/10.1016/j.saa.2013.10.104
21. P. Politzer and R.G. Parr, *J. Chem. Phys.*, **61**, 4258 (1974); https://doi.org/10.1063/1.1681726
22. P. Politzer, M.C. Concha and J.S. Murray, *Int. J. Quantum Chem.*, **80**, 184 (2000); https://doi.org/10.1002/1097-461X(2000)80:2<184::AID-QUA12>3.0.CO;2-O
23. B. Kramer, M. Rarey and T. Lengauer, *Proteins*, **37**, 228 (1999); https://doi.org/10.1002/(SICI)1097-0134(19991101)37:2<228::AID-PROT8>3.0.CO;2-8
24. S. Parveen, M.A. Al-Alshaikh, C.Y. Panicker, A.A. El-Emam, B. Narayana, V.V. Saliyan, B.K. Sarojini and C. Van Alsenoy, *J. Mol. Struct.*, **1112**, 136 (2016); https://doi.org/10.1016/j.molstruc.2016.02.018